American Journal of Engineering Research (AJER)
e-ISSN: 2320-0847 p-ISSN : 2320-0936
Volume-13, Issue-6, pp-15-30
www.ajer.org
Research Paper Open Access

Heat Transfer through an Impulsively Started Porous Limiting Surface in Hydromagnetic Oscillatory Flow

Okedoye M.Akindeleand Ogboru O. Kelvin
Department of Mathematics, Federal University of Petroleum Resources, Effurun, (NIGERIA),

ABSTRACT:*In this paper we have studied analytically the relationship between oscillatory free stream flow and two-dimensional hydromagnetic oscillatory flows of a viscous, incompressible, and electrically conducting fluid past a porous, infinite limiting surface, as well as the temperature and magnetic fields that are associated with these flows. Both frequency-dependent effects and "long-time" effects, which call for impractically long channels to be observed in steady flow is studied with oscillating fluid. For many industrial processes, it is essential to comprehend the physics of oscillating flows of complex fluids in small channels. Many chemical and biochemical engineering operations depend on effective fluid mixing and efficient mass and energy transport. Our analysis was carried out using semi-analytical method in the neighborhood of epsilon. From the result obtained, we discovered that that variation of transient velocity is the same with those of the mean velocity. Also, the mean velocity increases when the limiting surface moves in the positive direction of the flow, whereas it decreases when it moves in the opposite direction and increase in magnetic parameter decreases the mean velocity and that the magnetic field is limited to only retardation. Other flow governing parameters were displayed using graphs and discussed accordingly*

KEYWORDS Hydromagnetic, oscillation, limiting surface, magnetic field, suction, current density, porous, impulsively, electric current density*.*

Date of Submission: 25-05-2024 Date of acceptance: 06-06-2024

I. INTRODUCTION

For many industrial processes, it is essential to comprehend the physics of oscillating (or transient) flows of complex fluids in small channels. The quasi-periodic blood flow in the cardiovascular system can be described by the frequency components of the pressure and flow rate pulses, and many vascular diseases are associated with disturbances of the local flow conditions in the blood vessels. Understanding the physics of oscillating (or transient) flows of complex fluids in small channels is crucial for many industrial processes. The quasi-periodic blood flow in the cardiovascular system, characterized by the frequency components of pressure and flow rate pulses, highlights the significance of local flow conditions, which are often disrupted in various vascular diseases [1]. This understanding extends to diverse industrial applications, such as wastewater treatment, biofuel and fine chemical production, and bioprocessing [2,3]. In aerodynamics, it is relevant for fluttering airfoils and helicopter rotor dynamics [4].

Technical applications, such as inkjet printing, often require a rapid switch between "flow" and "no flow" of non-Newtonian fluids in small channel geometries. The typically low Reynolds numbers and the interaction between channels and macromolecules in such flows can lead to unique effects not seen in macroscopic systems [5]. Oscillatory flow is particularly beneficial for mixing immiscible phases or managing slurries, making it valuable in the production of biofuels, fine chemicals, and wastewater treatment [6].

Effective fluid mixing and efficient mass and energy transport are critical in many chemical and biochemical engineering operations. These conditions can be achieved through high-velocity turbulent flow in tubes or mechanical agitation in vessels. Alternatively, superimposing oscillatory flow on steady flow in a tube with periodic, sharp-edged baffles can enhance mixing within a tube [7]. This mixingmethod can lead to specific process improvements, including enhanced mass and heat transfer and reduced residence time [8]

NOMENCLATURE

x, y	spartial coordinate
U_0	mean free-stream velocity
U_1	velocity of the limiting surface
$U(t)$	free-stream velocity
u, v	velocity component in the x and y directions
$u(y,t)$	velocity field
$H(y,t)$	induced magnetic field
$\theta(y,t)$	temperature distribution
$u(y)$	transient velocity,
$H(y)$	transient induced magnetic field
$\theta(y)$	transient temperature.
t	time,
σ	electrical conductivity of the fluid,
μ_0	magnetic permeability,
υ	kinematic coefficient of viscousity
p	pressure
ρ	density.
H_0	externally applied transverse magnetic field
v_0	constant mean velocity,
A and ϵ	small positive constants such that $\epsilon A \ll 1$
ω	frequency of free – stream oscillation.
P_m	magnetic Prandtl number
$u_1(y)$	mean velocity
$H_1(y)$	mean induced magnetic
$\theta_1(y)$	mean temperature field
$u_2(y)$	mean oscillatory part of the velocity
$H_2(y)$	oscillatory part of the induced magnetic
$\theta_2(y)$	temperature field respectively
τ	skin friction
Z	electric current density
Nu	Nusselt number
T	fluid temperature
T_∞	free stream temperature
M	Hartmann number
Q	heat generation coefficient
c_p	specific heat at constant pressure
T_w	surface temperature

Dimensionless Group

Grt	thermal Grashof number
Pr	Prandtl number

Greek Letters

θ	non - dimensional fluid temperature
δ	heat generation/absorption

Subscripts

w	condition on the wall
∞	ambient condition

Both [9] and [10] studied this issue for constant suction, looking at the effects of free stream oscillation on the flow past an infinite porous limiting surface. The infinite limiting surface was assumed to be stationary in these investigations. Messiha's problem was expanded upon by [11],
who investigated how the oscillatory free stream affected the flow past an infinite porous limiting surface that was moving impulsively at a constant speed and had variable suction. According to [12], the topic of MHD has recently drawn a lot of academic attention due to both its own interest and its potential applications to astrophysics, geophysics, and engineering. According to [13]. The Velocity field in Hydromagnetic Oscillatory flow past an Impulsively Started Porous Limiting Surface with Variable Suction was studied. For the magnetic Prandtl number Pm=1 and the magnetic parameter $M < 1$, approximative solutions were found for the velocity field and expressions were given for the velocity, induced magnetic field, skin friction, and electric current density. The emerging flow parameters were examined and discussed when[14] considered confined swirling jet impingement onto an adiabatic wall. Recently, the entropy generation caused by heat transfer and fluid friction on a porous plate for the conjugate problem of an electrically conducting fluid in the presence of a strong magnetic field was considered by [15]. We looked into and talked about the effects of flow parameters on total entropy generation. How temperature-dependent thermal conductivity affected MHD free convection flow along a vertical flat plate was investigated [16]. Expression for entropy generation were obtained in their paper of [17], Second Law Analysis of Mass Transfer Effect on Unsteady MHD Flow Past an Accelerated Vertical Porous Plate. According to their findings, entropy is significantly influenced by magnetic parameter, heat generation, reaction type, mass Grashof number, and permeability parameter.Other recent work in this area includes the following, [18, 19, 20, 21, 22].

Heat and mass transfer in two-dimensional hydromagnetic oscillatory flow of a viscous, incompressible, and electrically conducting fluid past a porous, infinite surface have not been properly studied. This work aims to analyze the relationship between oscillatory free stream flow and such hydromagnetic flows with variable suction. It also examines the associated temperature and magnetic fields in the presence of a uniform transverse magnetic field. Oscillating fluid allows for the study of both frequency-dependent and long-term effects that require impractically long channels in steady flow.

II. FORMULATION OF THE PROBLEM

Considered is the two-dimensional hydromagnetic oscillating flow of a viscous, incompressible, electrically conducting fluid past an infinitely porous limiting surface with variable suction, such as the surface of a star. The x -axis is chosen along the limiting surface in the direction of the flow and the y -axis is taken

normal to the limiting surface. In the presence of a transverse magnetic field, the fluid limiting surface moves impulsively, at a constant speed, either in the direction of the flow or in the opposite direction. Because the induced magnetic field in the region under consideration is not insignificant, $H = (H_x, H_y, 0)$. Initially, the plate and the fluid are at same temperature $T_w$in a stationary condition with velocity U_0 at all points. At time t> 0 the plate starts oscillating in its own plane with a velocity U_1, Its temperature is raised to$e^{i\omega t}$.Within the framework of these assumptions using Boussinesq's approximation, the hydromagnetic flow relevant to the problem in the neighborhood of the plate is governed by the set of equations

$$\frac{\partial v}{\partial y} = 0 \tag{1}$$

$$\frac{\partial u}{\partial t} + v\frac{\partial u}{\partial y} = -\frac{1}{\rho}\frac{\partial p}{\partial x} + v\frac{\partial^2 u}{\partial y^2} + g\beta_T(T - T_\infty) + \frac{\mu_0}{\rho}H_y\frac{\partial H_x}{\partial y} \tag{2}$$

$$\frac{\partial H_x}{\partial t} + v\frac{\partial H_x}{\partial y} = \frac{1}{\sigma\mu_0}\frac{\partial^2 H_x}{\partial y^2} + H_y\frac{\partial u}{\partial y} \tag{3}$$

$$\rho C_p\left(\frac{\partial T}{\partial t} + v\frac{\partial T}{\partial y}\right) = k\frac{\partial^2 T}{\partial y^2} + Q(T - T_\infty) \tag{4}$$

The initial and boundary conditions are equally given by:

$$\left.\begin{array}{l} u = U_0, v = v_w(t), T = T_w, forally, t \le 0 \\ u = U_1, H_x = 0, H_x = 0, T = T_\infty + A, y = 0, t > 0 \\ u \to U(t), H_x = 0, T = T_\infty, asy \to \infty, t > 0 \end{array}\right\} \tag{5}$$

where all the parameter has their usual meaning as detailed in the nomenclature.

In accordance with Messiha[10], Equation (1) should integrate to:

$$v = -v_0(1 + \epsilon A e^{i\omega t}) \tag{6}$$

A and ϵ are small positive constants such that $\epsilon A \ll 1$.

In the free stream, $u = U(t)$, thus Equation (2) becomes

$$-\frac{1}{\rho}\frac{\partial p}{\partial x} = \frac{\partial U}{\partial t} \tag{7}$$

Also from Maxwell's equations the component of the electric current density are given by

$$\xi_x = 0, \quad \xi_y = 0$$

and

$$\xi_z = -\left(\frac{\partial H_x}{\partial y}\right) \tag{8}$$

And the divergence equation for the magnetic field gives

$$H_y = H_0 = \text{constant} \tag{9}$$

Let us introduce the non-dimensional variables:

$$\left.\begin{array}{l} y' = \frac{yv_0}{v}, u' = \frac{u}{U_0}, t' = \frac{tv_0^2}{4v}, U' = \frac{U}{U_0}, \omega' = \frac{4\omega v}{v_0^2}, V = \frac{U_1}{U_0} \\ H = (\frac{\mu_0}{\rho})^{\frac{1}{2}}\frac{H_x}{U_0}, \theta = \frac{T - T_\infty}{T_w - T_\infty}, M = (\frac{\mu_0}{\rho})^{1/2}\frac{H_0}{v_0} Pm = \sigma\mu_0 v \end{array}\right\} \tag{10}$$

Using the non-dimensional quantities (10) and equations (6)–(9), then equations (1) – (5) becomes

$$\frac{1}{4}\frac{\partial u}{\partial t} - (1 + \varepsilon A e^{i\omega t})\frac{\partial u}{\partial y} = \varepsilon\frac{i\omega}{4}e^{i\omega t} + \frac{\partial^2 u}{\partial y^2} + Grt\theta + M\frac{\partial H}{\partial y} \tag{11}$$

$$\frac{1}{4}\frac{\partial H}{\partial t} - (1 + \varepsilon A e^{i\omega t})\frac{\partial H}{\partial y} = \frac{1}{P_m}\frac{\partial^2 H}{\partial y^2} + M\frac{\partial u}{\partial y} \tag{12}$$

$$\frac{1}{4}\frac{\partial \theta}{\partial t} - (1 + \varepsilon A e^{i\omega t})\frac{\partial \theta}{\partial y} = \frac{1}{P_r}\frac{\partial^2 \theta}{\partial y^2} + \delta\theta \tag{13}$$

And the corresponding initial-boundary condition becomes

$$\left.\begin{array}{l} y = 0: u = V, H = 0, \theta = 1 \\ y \to \infty: u \to U, H \to 0, \theta \to 0 \end{array}\right\} \tag{14}$$

where

$$P_r = \frac{\mu c_p}{k}, \delta = \frac{Qv}{v_0^2\rho c_p}, P_m = \sigma\mu_0 v,$$

$$M = \left(\frac{\mu_0}{\rho}\right)^{\frac{1}{2}}\frac{H_0}{v_0}, Grt = \frac{vg\beta_\tau(T_w - T_\infty)}{U_0 v_0^2}$$

III. METHOD OF SOLUTION

To solve equations (11) – (13) with the initial boundary conditions (14), we use perturbation in the neighborhood of the limiting surface, similar to the one used by Lighthill[22]. The Velocity, induced magnetic and temperature fields are given by the expressions

$$u(y,t) = u_1(y) + \varepsilon A e^{i\omega t} u_2(y) \quad (15)$$

$$H(y,t) = H_1(y) + \varepsilon A e^{i\omega t} H_2(y) \quad (16)$$

$$\theta(y,t) = \theta_1(y) + \varepsilon A e^{i\omega t} \theta_2(y) \quad (17)$$

The stream velocity is given by

$$U(t) = 1 + \varepsilon e^{i\omega t} \quad (18)$$

Substituting equations 15, 16 and 17 into 11, 12, and 13 together with equation (18) respectively, separating the harmonic and non-harmonic terms and neglecting the coefficient of ε^2, we then obtain

$$u_1'' + u_1' + MH_1' = -Grt\theta_1 \quad (19)$$

$$\frac{1}{P_m} H_1'' + H_1' + Mu_1' = 0 \quad (20)$$

$$\frac{1}{P_r} \theta_1'' + \theta_1' + \delta\theta_1 = 0 \quad (21)$$

$$u_2'' + u_2' - \frac{i\omega}{4} u_2 = -\frac{i\omega}{4} - Au_1' - MH_2' - Grt\theta_2 \quad (22)$$

$$\frac{1}{P_m} H_2'' + H_2' - \frac{i\omega}{4} H_2 + Mu_2' = AH_1' \quad (23)$$

$$\frac{1}{P_r} \theta_2'' + \theta_2' + (\delta - i\omega)\theta_2 = -\theta_1' \quad (24)$$

Also the corresponding initial-boundary conditions are given by the expressions:

$$\left.\begin{array}{ll} y = 0: u_1 = V, u_2 = 0, & H_1 = 0, H_2 = 0, \theta_1 = 1, \theta_2 = 0 \\ y \to 0: u_1 \to 1, u_2 \to 1, & H_1 \to 0, H_2 \to 0, \theta_1 \to 0, \theta_2 \to 0 \end{array}\right\} \quad (25)$$

Without loss of generality, we choose magnetic prandtl number to be 1.

The solutions of Equations 19 – 24 under the boundary conditions (25) when $v = \alpha$ and magnetic parameter $M < 1$ are

$$\theta_1(y) = e^{-my} \quad (26)$$

$$H_1(y) = a_2 e^{-\alpha y} + a_3 e^{-\beta y} + a_4 e^{-my} \quad (27)$$

$$u_1(y) = 1 + a_2 e^{-\alpha y} - a_3 e^{-\beta y} + a_5 e^{-my} \quad (28)$$

$$\theta_2(y) = e^{-my} + ia_1(e^{-my} - e^{-m_1 y}) \quad (29)$$

$$H_2(y) = \frac{1}{2}\left[a_6 e^{-cy} + a_7 e^{-dy} + i\left(a_8 e^{-\alpha y} + a_{11} e^{-\beta y}\right) + (a_9 + a_{12})e^{-my} + (a_{10} + a_{13})e^{-m_1 y}\right] \quad (30)$$

$$u_2(y) = 1 + \frac{1}{2}\left[a_6 e^{-cy} - a_7 e^{-dy} + i\left(a_8 e^{-\alpha y} + a_{11} e^{-\beta y}\right) + (a_9 - a_{12})e^{-my} + (a_{10} - a_{13})e^{-m_1 y}\right] \quad (31)$$

We now substitute (26)-(31) into equations (19)-(21) respectively, we obtain the expression for the velocity, induced magnetic field and temperature distribution as

$$u(y,t) = 1 + \frac{V-1}{2}\left(e^{-\alpha y} - e^{-\beta y}\right) + \frac{Grt}{2m}\left(\frac{e^{-\alpha y}}{m-\alpha} + \frac{e^{-\beta y}}{m-\beta} - \frac{2Me^{-my}}{(m-\alpha)(m-\beta)}\right) + \frac{\varepsilon}{2} e^{i\omega t}\left(2 + (a_6 e^{-cy} - a_7 e^{-dy} + i\left(a_8 e^{-\alpha y} - a_{11} e^{-\beta y}\right) + (a_{14} + ia_{15})e^{-my} + (a_{10} - a_{13})e^{-m_1 y}\right) \quad (32)$$

$$H(y,t) = \frac{V-1}{2}\left(e^{-\alpha y} - e^{-\beta y}\right) + \frac{Grt}{2m}\left(\frac{e^{-\alpha y}}{m-\alpha} - \frac{e^{-\beta y}}{m-\beta} - \frac{2Me^{-my}}{(m-\alpha)(m-\beta)}\right) + \frac{\varepsilon}{2} e^{i\omega t}\left(a_6 e^{-cy} + a_6 e^{-dy} + i\left(a_8 e^{-\alpha y} + a_{11} e^{-\beta y}\right) + (a_9 + ia_{12})e^{-my} + (a_{10} + a_{13})e^{-m_1 y}\right) \quad (33)$$

$$\theta(y,t) = e^{-my} + i\varepsilon a_1 e^{i\omega t}(e^{-my} - e^{-m_1 y}) \quad (34)$$

Equations (32), (33) and (34) are split into pairs of real and imaginary parts.

From equation (32), the real part of the velocity can be written in terms of the fluctuating parts as

$$\Re\left(u(y,t)\right) = 1 + \frac{V-1}{2}\left(e^{-\alpha y} - e^{-\beta y}\right) + \frac{Grt}{2m}\left(\frac{e^{-\alpha y}}{m-\alpha} + \frac{e^{-\beta y}}{m-\beta} - \frac{2Me^{-my}}{(m-\alpha)(m-\beta)}\right) + \varepsilon(u_1 \cos\omega t + u_2 \sin\omega t) \quad (35)$$

Or

$$\Re\big(u(y,t)\big) = 1 + \frac{V-1}{2}\left(e^{-\alpha y} - e^{-\beta y}\right) + \frac{Grt}{2m}\left(\frac{e^{-\alpha y}}{m-\alpha} + \frac{e^{-\beta y}}{m-\beta} - \frac{2Me^{-my}}{(m-\alpha)(m-\beta)}\right) + \varepsilon|u_{12}|\cos(\omega t - \alpha_3)$$

Also from equation (33), the real part of the induced magnetic field can be written as

$$\Re(H(y,t)) = \frac{V-1}{2}\left(e^{-\alpha y} - e^{-\beta y}\right) + \frac{Grt}{2m}\left(\frac{e^{-\alpha y}}{m-\alpha} - \frac{e^{-\beta y}}{m-\beta} - \frac{2Me^{-my}}{(m-\alpha)(m-\beta)}\right) + \varepsilon(H_1\cos\omega t - H_2\sin\omega t) \quad (36)$$

or

$$\Re\big(H(y,t)\big) = \frac{V-1}{2}\left(e^{-\alpha y} - e^{-\beta y}\right) + \frac{Grt}{2m}\left(\frac{e^{-\alpha y}}{m-\alpha} - \frac{e^{-\beta y}}{m-\beta} - \frac{2Me^{-my}}{(m-\alpha)(m-\beta)}\right) + \varepsilon|H_{12}|\cos(\omega t + \alpha_2)$$

And from (34) we obtain the expression for temperature field as

$$\Re(\theta(y,t)) = e^{-my} + \varepsilon(t_1\cos\omega t - t_2\sin\omega t) \quad (37)$$

Or $\Re\big(\theta(y,t)\big) = e^{-my} + \varepsilon|t_{12}|\cos(\omega t - \alpha_1)$

From Equations (35), (36) and (37) we obtain the expression for the transient velocity, transient induced magnetic field and transient temperature respectively, when $\omega t = \pi/2$, as

$$\Re\big(u(y,t)\big) = 1 + \frac{V-1}{2}\left(e^{-\alpha y} - e^{-\beta y}\right) + \frac{Grt}{2m}\left(\frac{e^{-\alpha y}}{m-\alpha} + \frac{e^{-\beta y}}{m-\beta} - \frac{2Me^{-my}}{(m-\alpha)(m-\beta)}\right) + \varepsilon u_2$$

$$\Re\big(H(y,t)\big) = \frac{V-1}{2}\left(e^{-\alpha y} - e^{-\beta y}\right) + \frac{Grt}{2m}\left(\frac{e^{-\alpha y}}{m-\alpha} - \frac{e^{-\beta y}}{m-\beta} - \frac{2Me^{-my}}{(m-\alpha)(m-\beta)}\right) - \varepsilon H_2$$

$$\Re\big(\theta(y,t)\big) = e^{-my} - \varepsilon t_2$$

Since we know the velocity distribution, we then calculate the wall temperature (skin friction) as

$$\tau = \frac{\tau'}{\rho U_0' v_0'} = \left.\frac{\partial u}{\partial y}\right|_{y=0}$$

$$= -a_2\alpha + a_3\beta - ma_5 - \frac{\varepsilon}{2}e^{i\omega t}\big(-a_6 c + a_7 d + i(-a_8\alpha + a_{11}\beta) - m(a_{14} + ia_{15}) - m_1(a_{10} - a_{13})\big)$$

In terms of amplitude and phase of the skin friction, we have

$$\Re(\tau) = -a_2\alpha + a_3\beta - ma_5 - \varepsilon(\tau_1\cos\omega t + \tau_2\sin\omega t)$$

Or

$$\Re(\tau) = -a_2\alpha + a_3\beta - ma_5 - \varepsilon|\tau_{12}|\cos(\omega t - \alpha_4)$$

$$\tau_1 = -\frac{1}{2}[b_{11}c_1 - a_{21}c_2 - b_{13}d_1 + a_{22}d_2 - ma_{14} - n_1a_{18} + n_2a_{19}]$$

$$\tau_2 = -\frac{1}{2}[a_{21}c_1 - a_{22}d_1 - b_{13}d_1 - n_2a_{18} - n_1a_{19} + a_{11}\beta + c_2b_{11} - d_2b_{13} - ma_{15} - a_8\alpha]$$

$$|\tau_{12}| = (\tau_1^2 + \tau_2^2)^{\frac{1}{2}}, \tan\alpha_4 = \frac{\tau_2}{\tau_1}$$

Also since we know the induced magnetic distribution, we then calculate the electric current density as

$$Z = \frac{\upsilon\xi_{Z'}}{U_0' v_0'}\left(\frac{\mu_0}{\rho}\right)^{\frac{1}{2}} = \frac{\partial H}{\partial y} = a_2\alpha e^{-\alpha y} + a_3\beta e^{-\beta y} + ma_4 e^{-my} + \frac{\varepsilon}{2}e^{i\omega t}(a_6 c e^{-cy} - a_7 d e^{-dy} + i\big(a_8\alpha e^{-\alpha y} + a_{11}\beta e^{-\beta y}\big) - m(a_{14} + ia_{15})e^{-my} - m_1(a_{10} - a_{13})e^{-m_1 y})$$

And in terms of amplitude and phase of electric current density, we have

$$\Re(Z) = a_2\alpha e^{-\alpha y} + a_3\beta e^{-\beta y} + ma_4 e^{-my} - \varepsilon(Z_1\cos\omega t - Z_2\sin\omega t)$$

Or

$$\Re(Z) = a_2\alpha e^{-\alpha y} + a_3\beta e^{-\beta y} + ma_4 e^{-my} + \varepsilon|Z_{12}|\cos(\omega t + \alpha_5)$$

$$Z_1 = -\frac{1}{2}[(b_{11}c_1 - a_{21}c_2)\cos c_2 y\, e^{-c_1 y} + (a_{21}c_1 + b_{11}c_2)\sin c_2 y\, e^{-c_1 y} + (b_{13}d_1 - a_{22}d_2)e^{-d_1 y}\cos d_2 y + (a_{22}d_1 - b_{13}d_1)\sin d_2 y\, e^{-d_1 y}]$$

$$Z_2 = -\frac{1}{2}\big[(a_{21}c_1 + b_{11}c_2)\cos c_2 y\, e^{-c_1 y} - (b_{11}c_1 - a_{21}c_2)\sin c_2 y\, e^{-c_1 y} + \big((a_{22}d_1 + b_{13}d_2)\cos d_2 y - (b_{11}c_1 - a_{21}c_2)\sin c_2 y\big)e^{-d_1 y} + \big((a_{17}n_1 + a_{16}n_2)\cos n_2 y + (a_{16}n_1 - a_{17}n_2)\sin n_2 y\big)e^{-n_1 y} - \big(a_8\alpha e^{-\alpha y} + a_{11}\beta e^{-\beta y} + ma_{12}e^{-my}\big)\big]$$

$$|Z_{12}| = (Z_1^2 + Z_2^2)^{\frac{1}{2}}, \tan\alpha_5 = \frac{Z_2}{Z_1}$$

Finally, expression for Nusselt number is written as

$$Nu = \frac{\partial\theta}{\partial y}\Big|_{y=0} = m - i\varepsilon a_1 e^{i\omega t}(-m + n_1 + in_2)$$

In terms of amplitude and phase of the skin friction, we have

$$\Re(Nu) = m + \varepsilon(a_1 n_2 \cos\omega t + a_1(-m + n_1)\sin\omega t)$$

or

$$\Re(Nu) = m + \varepsilon|Nu_{12}|\cos(\omega t - \alpha_6)$$
$$Nu_1 = a_1 n_2, \qquad Nu_2 = a_1(-m + n_1)$$
$$|Nu_{12}| = (Nu_1^2 + Nu_2^2)^{\frac{1}{2}}, \tan\alpha_6 = \frac{Nu_2}{Nu_1}$$

IV. DISCUSSION

The analytical simulations presented in this work has been conducted in order to study the effects free stream oscillation ω for suction parameter A, hartmann number M, thermal Grashof number Grt and limiting surface velocity V.We set out the discussion of this work for velocity, magnetic and temperature fields for various flow governing parameters viz: V, M, A, δ, Grt and ω.

a. Velocity Field

The mean velocity profiles f_1 are shown in Figures 1.1 – 1.3 for different values of heat parameter δ, limiting surface velocity V, Thermal Grashof number Grt and magnetic parameter M. It worth nothing that variation of transient with velocity δ, V and Grt are the same with those of the mean velocity. We observe that heat generation increases the mean velocity while heat absorption reduces the velocity as could be seen from Figure 1.1. From Figure 1.2, we see that the mean velocity increases when the limiting surface moves in the positive direction of the flow, whereas it decreases when it moves in the opposite direction. The effect of Thermal Grashof number was shown in Figure 1.3, from the Figure, we see that the velocity increases with increase in Thermal Grashof number for heating of the plate ($Grt > 0$), while for cooling of the plate ($Grt < 0$) resulted in reversed type of flow with velocity decreases as cooling of the plate increases.

The variations of fluctuating parts of the velocity profiles u_1 and u_2 are displayed in Figures 1.4 – 1.9. From Figure 1.4 we see that for all chosen values of parameters, there is a reverse type of flow when limiting surface moves in the direction opposite to that of the flow, and as ω increases, the fluctuating part u_1 the reversibility reduces until a steady state is reached where oscillation is less significant. In Figure 1.5 we see that u_1 increases with an increase in A. Maximum in u_1 occurs when $A > 0.2$. We have from 1.6, the effect of Thermal Grashof number variation on fluctuating parts u_1 and u_2 respectively. It could be seen that the flow pattern in both cases is the same but the point of reversibility in u_1 is closer to the surface than that of u_2. In both u_1 and u_2, velocity increases positively for an increase in thermal Grashof number in cooling of the plate and increases negatively for heating of the plate. Increase in free stream oscillation frequency reduces the fluctuating part u_2 as could be seen in Figure 1.7. We observe a shift in maximum with increase in δ for fluctuating part u_2 as seen in Figure 1.8. The maximum shift away from the surface with a reverse flow occurring for higher values of δ. Also from Figure 1.9 an increase in limiting surface velocity positive values of V is seen to brings about decrease in fluctuating part u_2, whereas an increase in V in the reverse direction leads to an increase u_2.

The amplitude of the velocity profiles $|u_{12}|$ are shown in Figures 1.10, in which we observe from the figure that as the suction parameter A increases, $|u_{12}|$ increase and maximum amplitude occurs when $A \geq 0.1$. The variation of amplitude $|u_{12}|$ with thermal Grashof number Grt is observed to increase with positive increase in Thermal Grashof number for cooling of the plate ($Grt < 0$), while for heating of the plate ($Grt > 0$) resulted in reversed type of flow with velocity decreases as cooling of the plate increases.

The variation of phase angle $\tan\Omega_3$ is shown in Figure 1.11 and Figure 1.12. We see that as frequency ω increases phase angle decreases while heat generation δ increase to spatial point $y > 1.5$ when increase in δ decreases the phase angle.

b. Magnetic Field

We displayed in Figures 2.1 and 2.2 the mean induced magnetic field, g_1. We see that as M increases, and for negative values of V, g_1 increases. For heating of the plate ($Grt > 0$), the mean induced magnetic induction decreases as Grt increases, while for cooling of the plate ($Grt < 0$), the mean induced magnetic field increases. The variation of transient induced magnetic field H are shown in Figures 2.3 for various values of suction parameter. We observed that as M or ω increases and for negative values of V leads to an increase in H. Also as A increases, the transient induced magnetic field decreases as shown in Figure 2.3.

The variations of the fluctuating parts H_1 and H_2 of the induced magnetic field are shown in Figures 2.4 – 2.10. From Figure 2.4, we observed that as Grt (for heating of the plate) increases, H_1 also increases,

while for cooling of the plate, increase in Grt leads to increase in H_1 and H_2, as increase in ω reduces the fluctuation while increase in ω reduces the fluctuation as seen in Figure 2.5. The amplitude $|H_{12}|$ of induced magnetic field is shown in Figure 2.6, it could be seen that the amplitude of induced magnetic field decreases with increase in heat absorption for $\delta < -1$and increase with with heat absorption for $\delta > -1$, while in Figures 2.7, we see that as frequency ω increase, fluctuating parts H_2 increases. Figure 2.8 shows that amplitude of induced magnetic field increase with an increase in thermal Grashof number for heating of the plate.

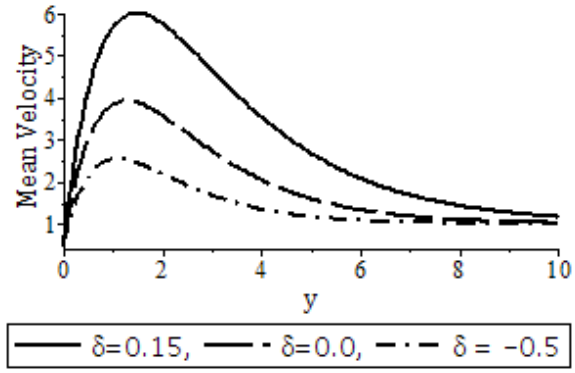

Figure 1.1: Mean velocity profiles (f_1) for various δ

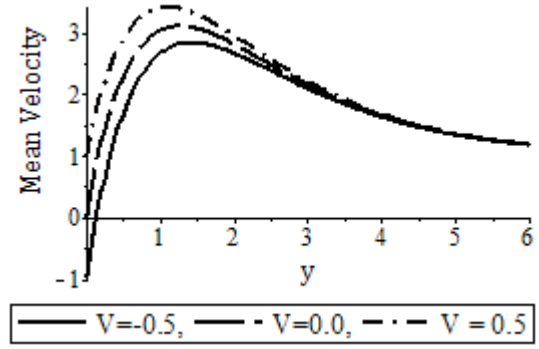

Figure 1.2: Mean velocity profiles (f_1) for various V

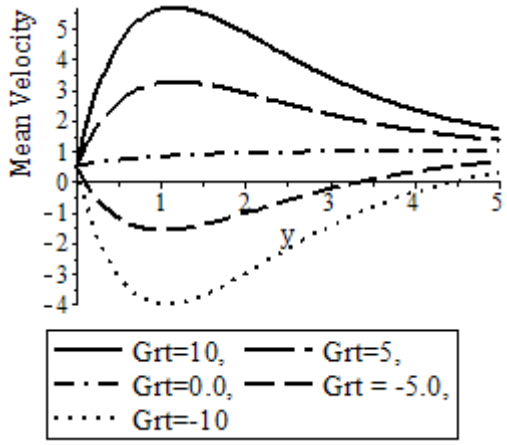

Figure 1.3: Mean velocity profiles (f_1) for various Grt

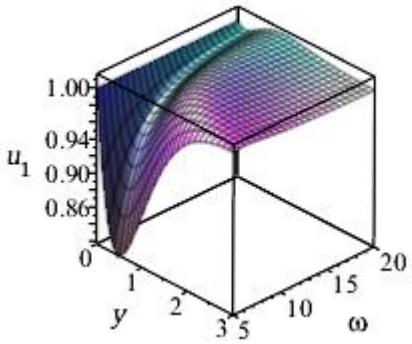

Figure 1.4: Fluctuating part of velocity profiles (u_1) for various ω

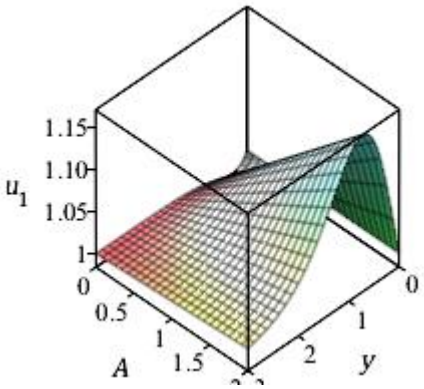

Figure 1.5: Fluctuating part of velocity profiles (u_1) for various A

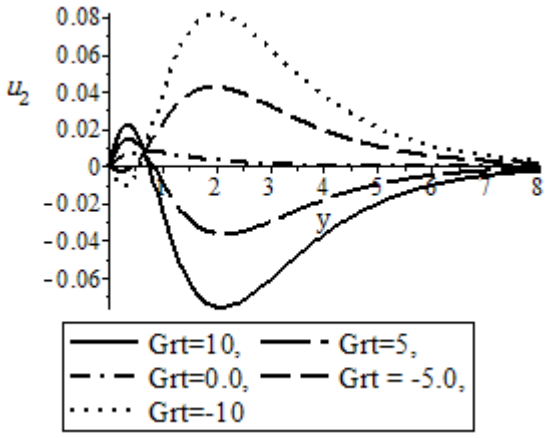

Figure 1.6: Fluctuating part of velocity profiles (u_2) for various Grt

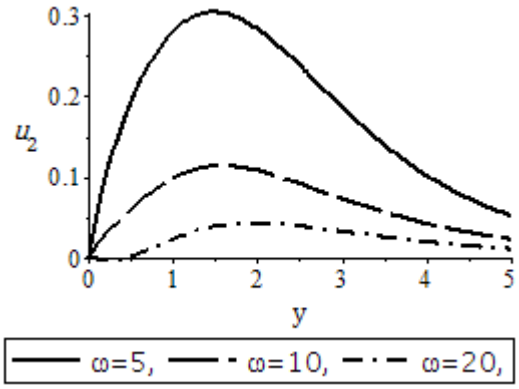

Figure 1.7: Fluctuating part of velocity profiles (u_2) for various ω

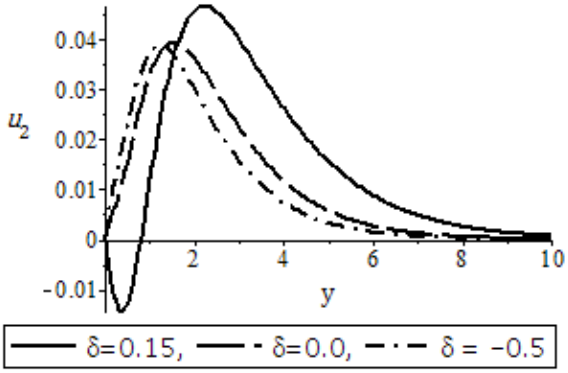

Figure 1.8: Fluctuating part of velocity profiles (u_2) profiles (u_1) for various δ

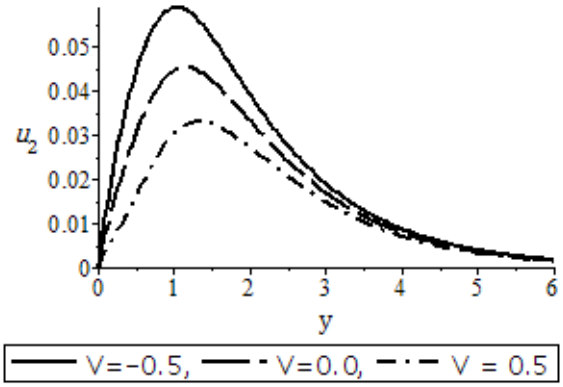

Figure 1.9: Fluctuating part of velocity profiles (u_1) for various V

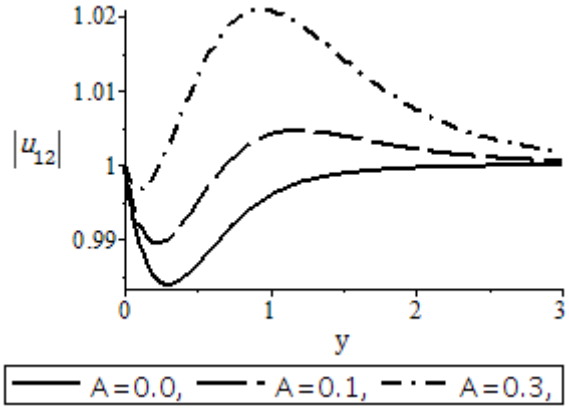

Figure 1.10: Amplitude of velocity profiles $(|u_{12}|)$ for various A

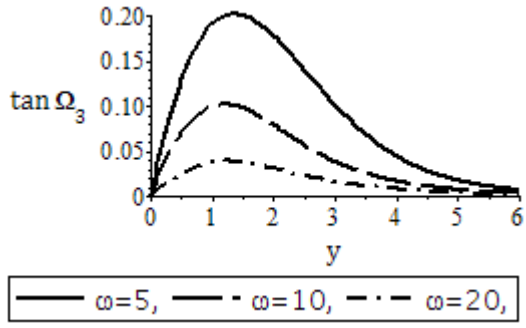

Figure 1.11: Phase of velocity $(\tan \Omega_3)$ profiles for various ω

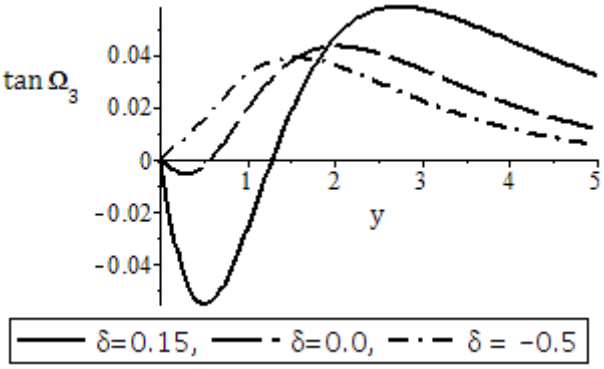

Figure 1.12: Phase of velocity $(\tan \Omega_3)$ profiles various δ

The variations of the fluctuating parts H_1 and H_2 of the induced magnetic field are shown in Figures 2.4 – 2.10. From Figure 2.4, we observed that as Grt (for heating of the plate) increases, H_1 also increases, while for cooling of the plate, increase in Grt leads to increase in H_1 and H_2, as increase in ω reduces the fluctuation while increase in ω reduces the fluctuation as seen in Figure 2.5. The amplitude $|H_{12}|$ of induced magnetic field is shown in Figure 2.6, it could be seen that the amplitude of induced magnetic field decreases with increase in heat absorption for $\delta < -1$and increase with with heat absorption for $\delta > -1$, while in Figures 2.7, we see that as frequency ω increase, fluctuating parts H_2 increases. Figure 2.8 shows that amplitude of induced magnetic field increase with an increase in thermal Grashof number for heating of the plate.

The phase of induced magnetic field is plotted for various values of frequency of the free stream oscillation ω, heat generation/absorption, suction parameter A and Hartmann number as shown in Figures 2.9 and 2.10. It could be deduced from the Figures that increase in A or M reduces the phase angle for reverse flow.

We also observed that phase change occurs at $y \to 2$, and when this happens the direction induced magnetic phase changes.

c. Temperature Field

In Figure 3.1, we display the transient temperature field with various values of δ. It is observed that temperature boundary layer decreases as the fluid moves away from the plate which asymptotically approaches zero far away from the plate and temperature increases as the fluid heat absorption increases.

Thus, the higher boundary layer occurs as heat generated to the surrounding reduces.

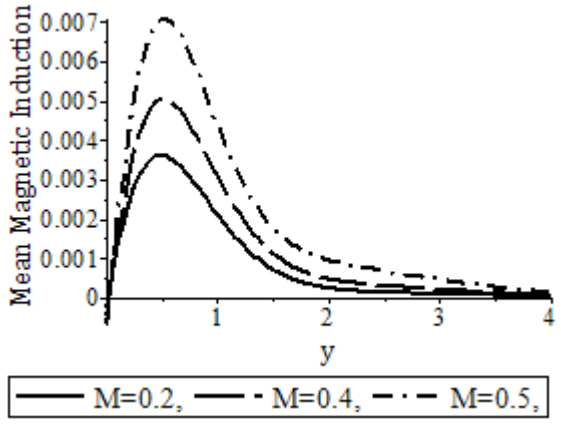

Figure 2.1: Mean induced magnetic field (g_1) for various M

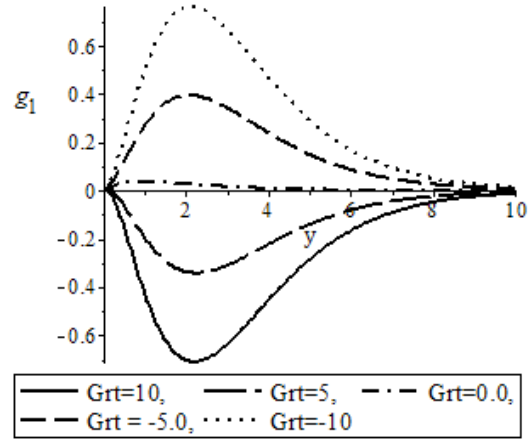

Figure 2.2: Mean induced magnetic field (g_1) for various Grt

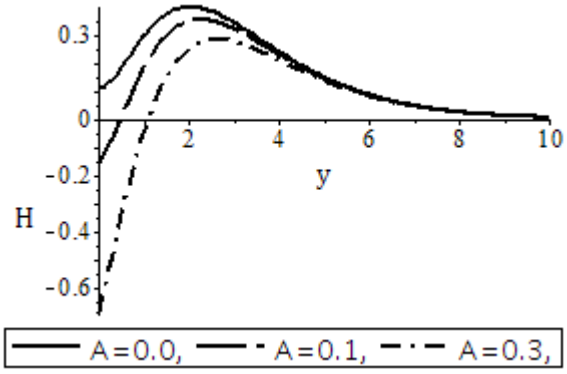

Figure 2.3: Transcient induced magnetic field (H) for various A

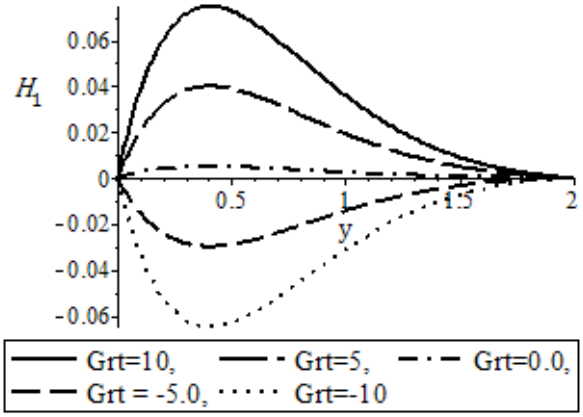

Figure 2.4: Fluctuating part of induced magnetic field (H_1) for various Grt

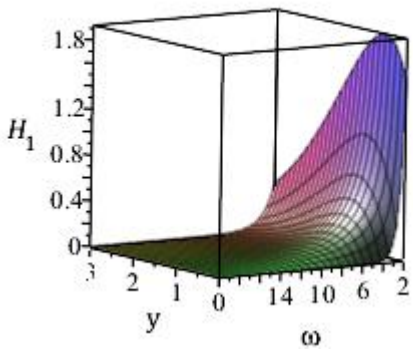

Figure 2.5: Fluctuating part of induced magnetic field (H_1) for various ω

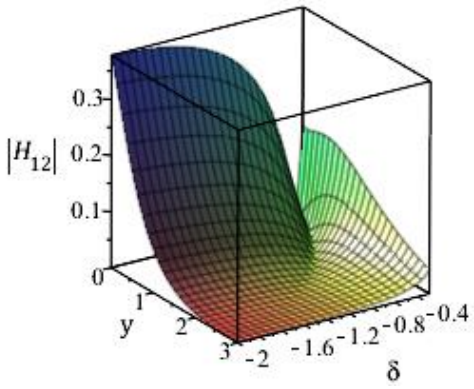

Figure 2.6: Amplitude of induced magnetic field $(|H_{12}|)$ for various δ

The amplitude of temperature field $|\theta_{12}|$ is shown in Figure 3.2, fluctuation due to θ_2 is seen to dominate. Amplitude of the temperature increases with an increase in heat generation up to around $y = 1.2$ after which it revserses. The effect of Hartmann number on Phase of temperature field for various $A(\tan\Omega_1)$ for various δ is shown in Figure 3.3. We observed that the phase angle also increases with increase heat generation, which also increses the interval of complete oscillations.

d. Skin Friction

The Skin Friction τ is plotted for against free stream oscillation ω for suction parameter A, hartmann number M, thermal Grashof number Grt and limiting surface velocity V in Figures 4.1 to 4.5 respectively. It is observed that τ decreases as A increase, whereas it increases as M increases, and also an increase in Grt increases τ. Also, τ decrease when limiting surface moves in the same direction as that of the flow and increase when the limiting surface moves in the direction opposite to that of the flow. The amplitude of the skin friction $|\tau_{12}|$ is shown in Figure 4.4. We observed that amplitude increase with an increase in Grt and A. The amplitude of the skin friction is highest close to the surface as against the surface. Also the amplitude is also higher when the plate moves in the opposite direction of the flow as compared to the amplitude when the plate moves in the same direction as the flow. The phase of the skin friction is shown in Figure 4.5 and 4.6 respectively. From this Figures, we observe that of the skin friction decreases when the limitin surface moves in the direction of the flow and increase when it moves in the opposite direction of the flow, while increase in M or ω reduces the phase of the skin friction.

E Electric Current Density

The variation of the electric current density Z, the fluctuation part Z_1, Z_2 the amplitude, $|Z_{12}|$ and the pahse, $\tan\alpha_5$ of the electric current density are displayed in Figures 5.1 to 5.7. From these Figures, we see that increase in heat absorption increases Z while increase in heat generation reduces the electric current density for $y < 2.5$, when $y > 2.5$, the phenomenon reverses. For heating of the plate, increase in Grt decreases Z while for cooling of the plate, increase in Grt increases Z. The electric current density flows in the positive direction when $0.5 < y < 1.5$ for heating of the plate and vice versa for cooling of the plate. It is also seen that as free stream oscillation frequency increase, the electric current density decreases. Close to the plate, the electric current density flow in the negative direction and as M increase Z decreases for $y < 3$ and reverses when $y > 3$. Z is seen to increase as A increase with Z in negative direction when $A < 0.2$ with $0 < y < 2$. The fluctuation part Z_2 increase with increase in heating of the plate and decreases with cooling of the plate. The amplitude decrease with increase in Grt or ω. The phase of the current density increase with heat generation but reverses as y increases with negative phase angle. The phase of current density decreases with increase in free stream oscillation. We also observe that the point of asymptotes increases as y becomes large with negative phase.

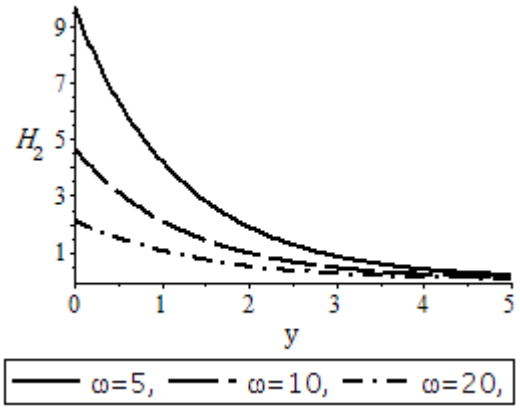

Figure 2.7: Fluctuating part of induced magnetic field (H_2) for various ω

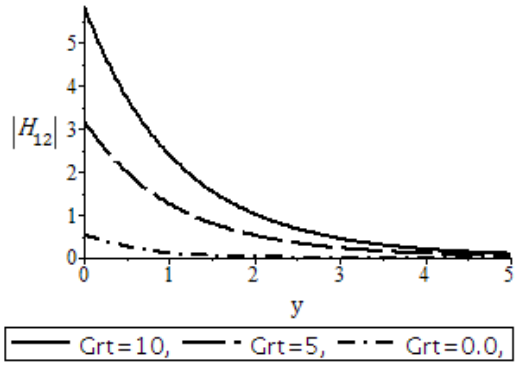

Figure 2.8: Amplitude of induced magnetic $(|H_{12}|)$ for various Grt

F Nusselt Number

The variation of rate of heat transfer at the wall Nu, its amplitude $|N_{12}|$ and phase $\tan\alpha_6$ are plotted in Figures 6.1 and 6.2 respectively. It is seen that increase in heat generation leads to increase in Nu and its amplitude. While the pahse of Nusselt number decreases as heat generation increases.

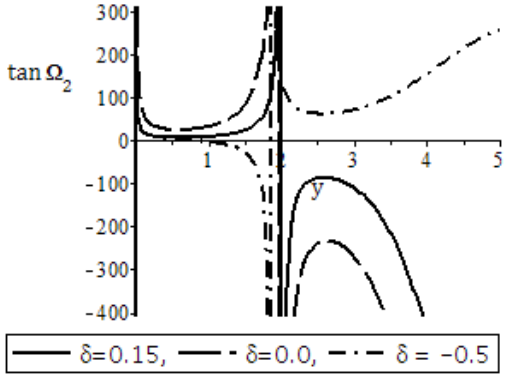

Figure 2.9: Phase of induced magnetic field ($\tan\Omega_2$) for various δ

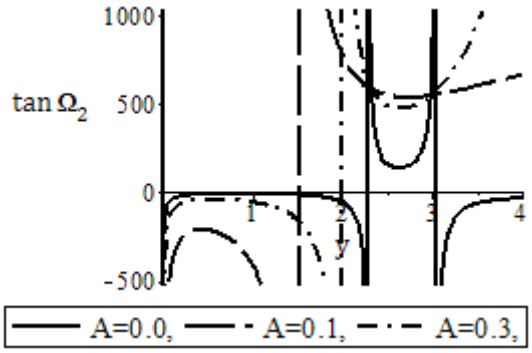

Figure 2.10: Phase of induced magnetic field ($\tan\Omega_2$) for various A

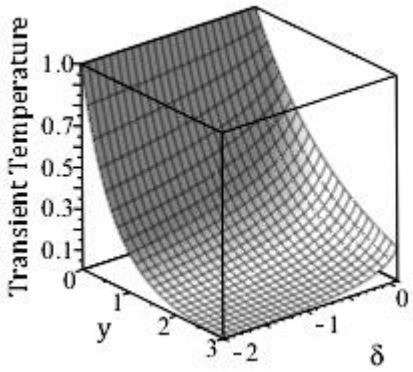

Figure 3.1: Transcient temperature field (θ) for various δ

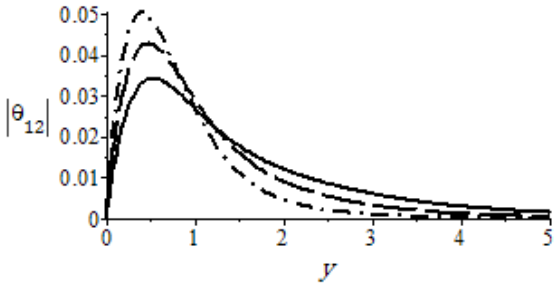

Figure 3.2: Amplitude of temperature field ($|\theta_{12}|$) for various δ

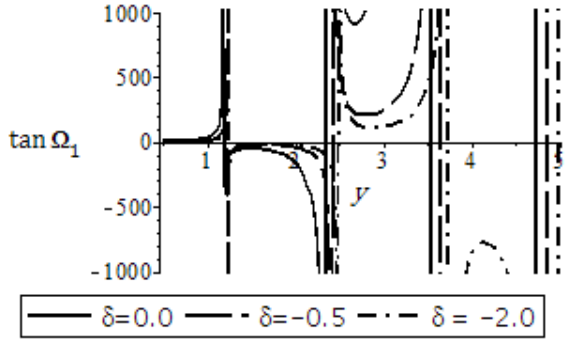

Figure 3.3: Phase angle for temperature field ($\tan\Omega_1$) for various δ

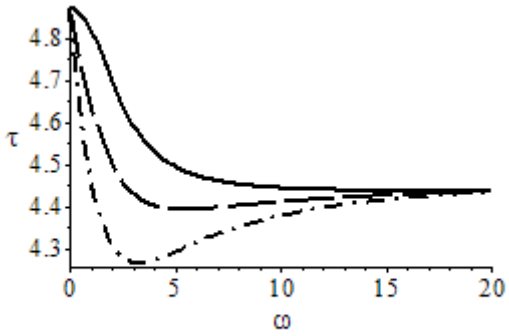

Figure 4.1 Variation of skin friction (τ) for various A

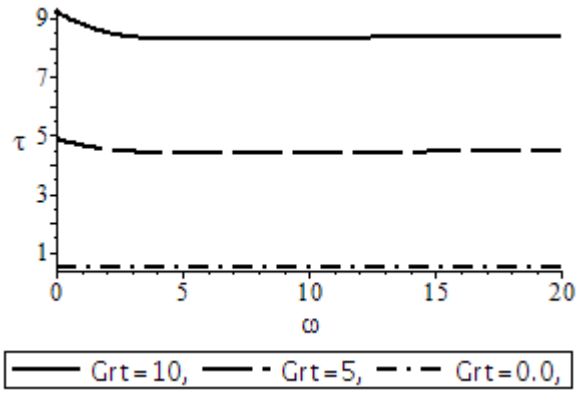

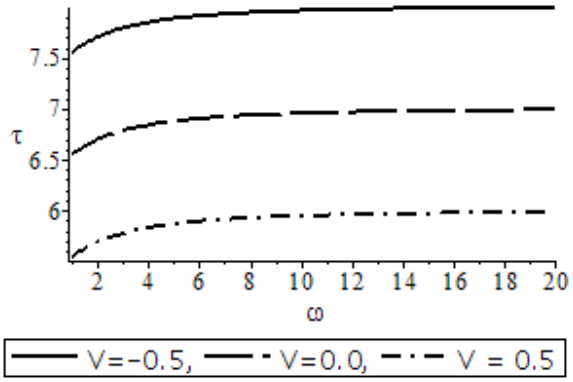

Figure 4.2: Variation of skin friction (τ) for various Grt

Figure 4.3: Variation of skin friction (τ) for various V

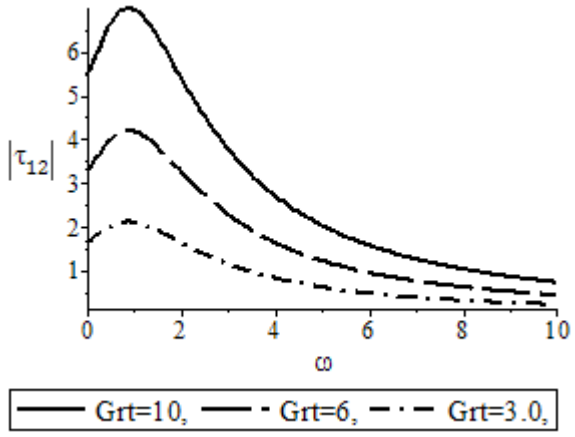

Figure 4.4: Amplitude of the skin friction $(|\tau_{12}|)$ for various Grt

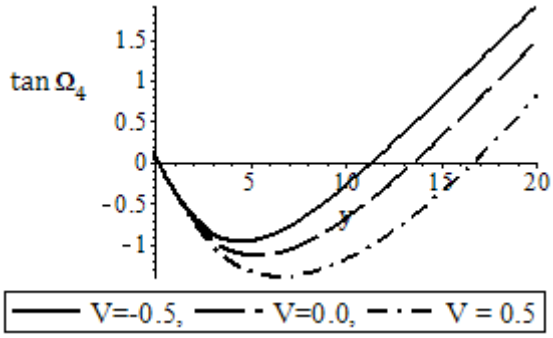

Figure 4.5: Phase of the skin friction $(\tan\Omega_4)$ for various V

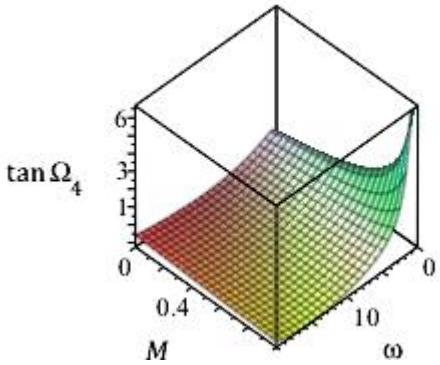

Figure 4.6: Phase of the skin friction $(\tan\Omega_4)$ as function of M and ω

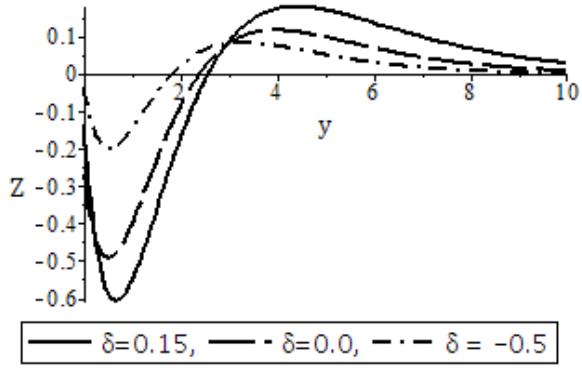

Figure 5.1: Electric current density (Z) for various δ

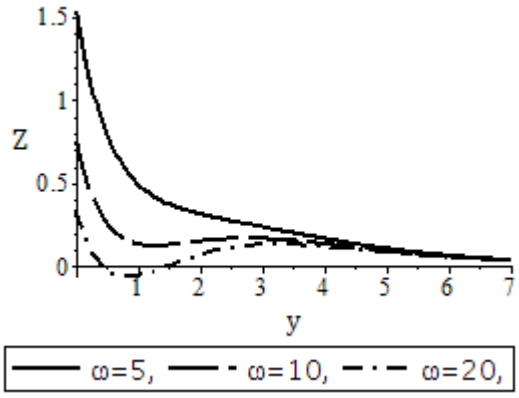

Figure 5.2: Electric current density (Z) for various ω

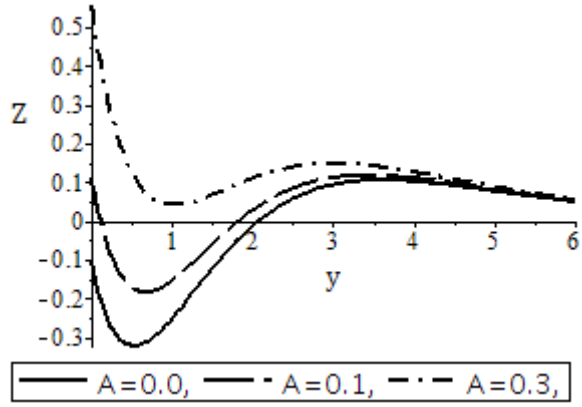

Figure 5.3: Electric current density (Z) for various A

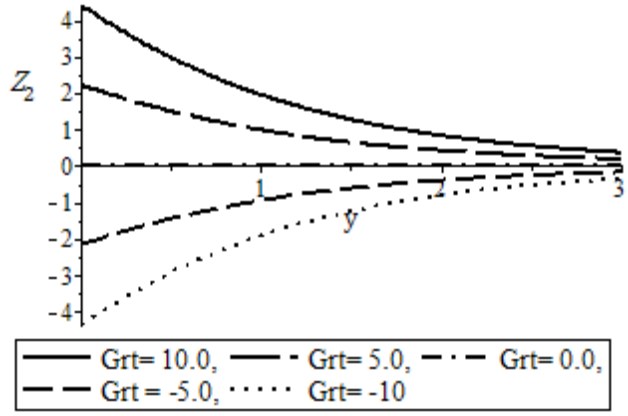

Figure 5.4: Fluctuation part of the electric current density (Z_2) for various Grt

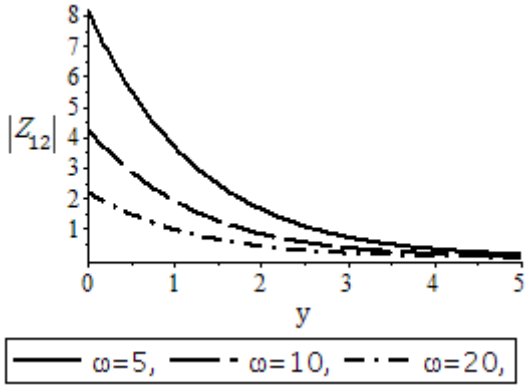

Figure 5.5: Amplitude of the electric current density $(|Z_{12}|)$ for various ω

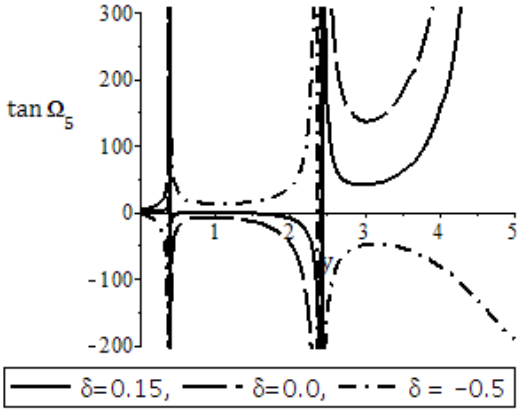

Figure 5.6: Phase of the electric current density $(\tan \Omega_5)$ for various δ

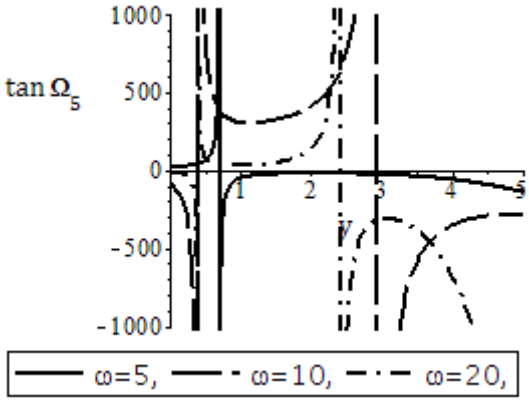

Figure 5.7: Phase of the electric current density $(\tan \Omega_5)$ for various ω

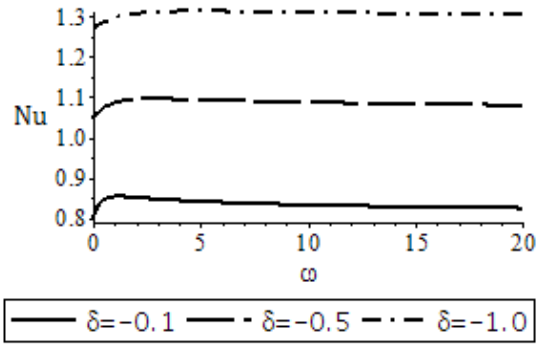

Figure 6.1: Variation of transcient Nusselt (Nu) for various δ

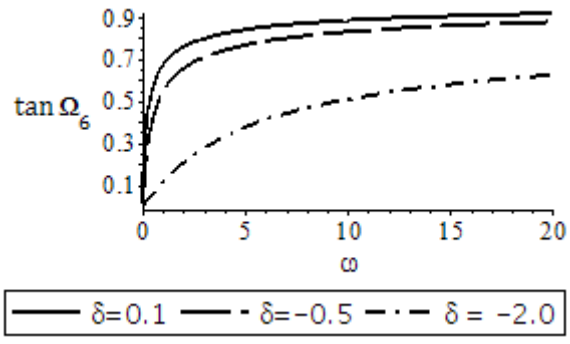

Figure 6.2: Phase of Nusselt number $(\tan \alpha_6)$ for various δ

V. CONCLUSIONS

In this paper we have studied analytically heat transfer in Hydromagnetic oscillatory flow past an impulsively started porous limiting surface and the corresponding effect of oscillatory free stream flow on two dimensional hydromagnetic oscillatory flows of a viscous, incompressible and electrically conducting fluid, past a porous, infinite limiting surface with variable suction and its associated temperature and magnetic fields in the presence uniform transverse magnetic field. The fluid limiting surface is moved impulsively, with a constant velocity, either in the direction of the flow or in the opposite direction, in the presence of a transverse magnetic field. With oscillating fluid flow, we can study both frequency-dependent effects and "long-time" effects that would require non-practically long channels to be observed in steady flow.

We explore mathematically important aspects of reaction engineering in oscillatory flow, especially residence time flow behaviour, scale-up and scale-down procedures.

Oscillatory Flow Mixing can be applied to both batch and continuous processing, such as in chemical, biochemical and process engineering.

The method of mixing provides a range of specific process enhancements, such as improved mass transfer, heat transfer, and narrow residence time, Significant enhancement of heat and mass transfer rates, Control of droplets/bubble size and size distribution, Control of the Residence Time Distribution (RTD), Suspension of particles. Fine-tuned mixing and shear rates where mixing is controlled entirely by the oscillations and not by the throughput.

From the present study the following conclusions can be drawn:

- that variation of transient with velocity δ, V and Grt are the same with those of the mean velocity.
- that the mean velocity increases when the limiting surface moves in the positive direction of the flow, whereas it decreases when it moves in the opposite direction.
- that increase in magnetic parameter M decreases the mean velocity and that the magnetic field is limited to only retardation, as normal.
- that τ decrease when limiting surface moves in the same direction as that of the flow and increase when the limiting surface moves in the direction opposite to that of the flow.
- that amplitude of the skin friction is highest close to the surface as against the surface.
- that increase in heat absorption increases Z while increase in heat generation reduces the electric current density.
- that increase in heat generation leads to increase in Nu and its amplitude. While the pahse of Nusselt number decreases as heat generation increases.

Acknowledgements

The authors gratefully acknowledge the management team of Federal University of Petroleum Resources for allowing an enabling environment that support intensive research and also grateful to members of editorial board for their usual suggestions and idea that led to improvement of this work

References

[1]. Taylor, C. A., & Figueroa, C. A. (2009). Patient-specific modeling of cardiovascular mechanics. *Annual Review of Biomedical Engineering, 11*, 109-134.
[2]. Zhou, H., Meng, A., Long, Y., Li, Q., & Zhang, Y. (2019). An overview of characteristics of municipal solid waste fuel in China: Physical, chemical composition and heating value. *Renewable and Sustainable Energy Reviews, 36*, 107-122.
[3]. Sun, Z., & Liao, W. (2014). Bio-oil production and upgrading research: A review. *Renewable and Sustainable Energy Reviews, 40*, 793-804.
[4]. Lee, T., Su, Y. Y., & Fu, T. C. (2020). Aerodynamic optimization of rotor blades for wind turbines and helicopters: A review. *Renewable Energy, 147*, 2745-2760.
[5]. Bird, R. B., Armstrong, R. C., &Hassager, O. (1987). *Dynamics of Polymeric Liquids. Vol. 1: Fluid Mechanics*. Wiley-Interscience.
[6]. Brennen, C. E. (2005). *Fundamentals of Multiphase Flow*. Cambridge University Press.
[7]. Mackley, M. R., & Stonestreet, P. (1995). Heat transfer and associated energy dissipation for oscillatory flow in baffled tubes. *Chemical Engineering Science, 50*(14), 2211-2224.
[8]. Deshmukh, S. D., Bhopale, P. M., &Bhopale, S. M. (2017). Enhancement of heat transfer by using oscillatory flow: A review. *Heat and Mass Transfer, 53*(4), 1253-1268.
[9]. Stuart, J.T. (1955): "A solution of the Navier–Stokes and energy equations illustrating the response of skin friction and temperature of an infinite plate thermometer to fluctuations in the stream velocity", Proceedings of The Royal Society of London. Series A, 231(1184), pp. 116–130. https://doi.org/10.1098/rspa.1955.0160.
[10]. Messiha S.A.S. (1966): Laminar Boundary Layers in Oscillatory Flow along an Infinite Flate Plate with Variable suction, Proc. Camb. Phil. Soc. 62, pp.329-337. https://doi.org/10.1017/S030500410003989X
[11]. Soundalgekar, V. (1979). Free convection effects on the flow past a vertical oscillating plate,. Astrophysics and Space Science, 64, 165 - 172. https://doi.org/10.1007/BF00640038.
[12]. Cramer, K. R., & Shih, P. (1973). Magnetofluid Dynamics for engineers and Applied Physicists. New York: McGraw-Hill Book Company.
[13]. Georgantopoulos, G. A., Douskos, C. N., Vassios, G. L. and Katsiaris, G. A. (1979): The Velocity field in Hydromagnectic Oscillatory flow past an Impulsively Started Porous Limiting Surface with Variable Suction. Astrophysics and Space Science 63, 419-438, 0004-640X/79/0632-0419503.00.
[14]. Shuja, S.Z. Yilbas, B. S. and Rashid M. (2003): Confined swirling jet impingement onto an adiabatic wall. International Journal of Heat and Mass Transfer, 46, 29472955. https://doi.org/10.1016/S0017-9310(03)00073-5
[15]. Okedoye, A. M., &Ayandokun, O. O. (2013): Second law analysis of heat and hall effect of an oscillating plate in a Porous medium. . Asian Journal of Science and Technology, 4(7), 4 – 9.
[16]. Okedoye, A. M. (2014a). Second Law Analysis of Mass Transfer Effect on Unsteady MHD flow Past an Accelerated Vertical Porous Plate. International Journal of Pure and Applied mathematical Science and Technology, 24(2), 29 - 38
[17]. Okedoye, A. M. (2014b). Unsteady MHD mixed convection flow past an oscillating plate with heat source/sink. Journal of Naval Architecture and Marine Engineering 11(2014) 167-176., 11(1), 167 - 176. https://doi.org/10.3329/jname.v11i2.6477.
[18]. Lawal M. Muhammad, Ogboru O. Kelvin and **Okedoye M. Akindele (2024)**. Influence of Electric Field Flow on MHD Nano-Fluid Over a Stretching Sheet. American Journal of Engineering Research (AJER) e-ISSN: 2320-0847 p-ISSN: 2320-0936 Volume-13, Issue-4, pp-88-95 www.ajer.org.

[19]. Lawal M. Muhammad, Ogboru O. Kelvin and **Okedoye M. Akindele (2024)**. Heat and Mass Transfer Mixed Convective Electrically Conducting Nanomaterial Flow Over a Stretching Sheet. Journal of Multidisciplinary Engineering Science and Technology (JMEST) pp 16804 –16812,Vol. 11 Issue 4, April – 2024. ISSN: 2458-9403.JMESTN42354376
[20]. Sunday O. Olokor, Mathew O. Alabi and Akindele M. Okedoye (2024):Entropy Generation in Unsteady Oscillatory MHD Flow with Thermal Radiation and Binary Chemical Reaction.*International Journal of Computational Engineering Research (IJCER).* Volume, 14 || Issue, 3|| Page 58 - 71 May. - June. – 2024
[21]. Ometan, S.O., Alabi M.O. & Okedoye A.M. (2024). Analyzing the Impact of Heat and Mass Transfer on Unsteady MHD Flow with Thermal Radiation and Binary Chemical Reaction. *European Journal of Theoretical and Applied Sciences*, 2(3), 267-280. DOI: 10.59324/ejtas.2024.2(3).23
[22]. Lighthill M.J.: The response of laminar skin friction and heat transfer to fluctuations in the stream velocity, Proceeding of the royal society of London, A224, 1-23 (1954). https://doi.org/10.1098/rspa.1954.0049.

Appendix

A1: Parameters Definition/Expression

$$m=\frac{\Pr+\sqrt{\Pr^2-4\Pr\delta}}{2}, m_1=\frac{\Pr+\sqrt{\Pr^2-4(\delta-i\omega)}}{2}, c=\frac{\alpha+\sqrt{\alpha^2+i\omega}}{2}, d=\frac{\beta+\sqrt{\beta^2+i\omega}}{2}$$

$$1+M=\alpha, 1-M=\beta, m_1=n_1+in_2, c=c_1+ic_2, d=d_1+id_2, a_1=\frac{m}{\omega\Pr},$$

$$a_2=\frac{V-1}{2}+\frac{Grt}{2m(m-\alpha)}, a_3=-\left(\frac{V-1}{2}+\frac{Grt}{2m(m-\beta)}\right), a_4=-\frac{MGrt}{m(m-\alpha)(m-\beta)},$$

$$a_5=\frac{(1-m)Grt}{m(m-\alpha)(m-\beta)}, a_8=\frac{8A\alpha a_2}{\omega}, a_9=\frac{Am(a_4+a_5)+Grta_1}{m^2-\alpha m-\frac{i\omega}{4}}, a_{10}=\frac{-a_1Grt}{m_1^2-\alpha m_1-\frac{i\omega}{4}}$$

$$a_{11}=\frac{8A\beta a_3}{\omega}, a_{12}=\frac{Am(a_4-a_5)-Grta_1}{m^2-\beta m-\frac{i\omega}{4}}, a_{13}=\frac{a_1Grt}{m_1^2-m_1\beta-\frac{i\omega}{4}},$$

$$u_1=1-\frac{1}{2}[a_{14}e^{-my}-(b_{11}\cos c_2y+a_{21}\sin c_2y)e^{-c_1y}+(b_{13}\cos d_2y+a_{22}\sin d_2y)e^{-d_1y}+(a_{18}\cos n_2y+a_{19}\sin n_2y)e^{-n_1y}]$$

$$u_2=-\frac{1}{2}[a_8e^{-\alpha y}-a_{11}e^{-\beta y}+a_{15}e^{-my}+(b_{11}\sin c_2y-a_{21}\cos c_2y)e^{-c_1y}+(a_{22}\cos d_2y-b_{13}\sin d_2y)e^{-d_1y}+(a_{19}\cos n_2y-a_{18}\sin n_2y)e^{-n_1y}]$$

$$|u_{12}|=(u_1^2+u_2^2)^{\frac{1}{2}}, \tan\alpha_3=\frac{u_2}{u_1}$$

$$H_1=\begin{bmatrix}a_9e^{-my}+(a_{16}\cos n_2y+a_{17}\sin n_2y)e^{-n_1y}-(b_{11}\cos c_2y+a_{21}\sin c_2y)e^{-c_1y}\\-(b_{13}\cos d_2y+a_{22}\sin d_2y)e^{-d_1y}\end{bmatrix}$$

$$H_2=\frac{1}{2}[a_8e^{-\alpha y}+a_{11}e^{-\beta y}+a_{21}e^{-my}+(a_{17}\cos n_2y-a_{16}\sin n_2y)e^{-n_1y}+(a_{11}\sin c_2y-a_{21}\cos c_2y)e^{-c_1y}+(b_{13}\sin d_2y-a_{22}\cos d_2y)e^{-c_1y}]$$

$$|H_{12}|=(H_1^2+H_2^2)^{\frac{1}{2}}, \tan\alpha_2=\frac{H_2}{H_1}$$

$$n_1=\frac{1}{2}Pr+n_2, n_2=\frac{1}{4}\sqrt{2(Pr^2-4Pr\delta)^2+16\omega^2Pr^2+2Pr^2-8Pr\delta}$$

$$a_{14}=\frac{b_1b_2}{{b_2}^2+\omega^2}-\frac{b_3b_4}{{b_4}^2+\omega^2}, a_{15}=\omega\left(\frac{b_1}{{b_2}^2+\omega^2}-\frac{b_3}{{b_4}^2+\omega^2}\right),$$

$$b_1 = 4Grt\left(\frac{A}{\alpha - m} + a_1\right), b_2 = 4(m - \alpha), b_3 = -4Grt\left(\frac{A}{\beta - m} + a_1\right),$$

$$b_4 = 4(m - \beta), b_5 = {n_1}^2 - {n_2}^2 - \alpha n_1, b_6 = 2n_1 n_2 - \alpha n_2 - \frac{i\omega}{4}, b_7 = {n_1}^2 - {n_2}^2 - \beta n_1,$$

$$b_8 = 2n_1 n_2 - \beta n_2 - \frac{i\omega}{4}, b_{11} = \frac{b_1 b_2}{{b_2}^2 + \omega^2} - \frac{a_1 b_5 Grt}{{b_5}^2 + {b_6}^2}, b_{12} = \frac{b_1 \omega}{{b_2}^2 + \omega^2} - \frac{a_1 b_6 Grt}{{b_4}^2 + b_6},$$

$$b_{13} = \frac{b_3 b_4}{{b_4}^2 + \omega^2} + \frac{a_1 b_7 Grt}{{b_7}^2 + {b_8}^2}, b_{14} = \frac{b_3 \omega}{{b_4}^2 + \omega^2} - \frac{a_1 b_8 Grt}{{b_7}^2 + {b_8}^2}$$

$$t_1 = a_1 \sin n_2 y\, e^{-n_1 y}, t_1 = a_1(e^{-my} - \cos n_2 y\, e^{-n_1 y})$$

$$|t_{12}| = (t_1^2 + t_2^2)^{\frac{1}{2}}, \tan \alpha_1 = \frac{t_2}{t_1}$$